Although we know of no general argument that requires the off-diagonal matrix elements of $A_1(\alpha)$ to be zero, for states of equal energy, as above, we have been unable to find any example of a choice of $A_1(\alpha)$ and $H_{0,i}$ where these off-diagonal elements are different from zero. When they are zero, (16) simplifies: The sum over b' contains only the term $b'=b$.

The limitation that $A_1(\alpha)$ be in an eigenstate initially is clearly less general than it need be, for it is physically possible to measure the expectation value of an observable in any initial state—not necessarily an eigenstate—and then to observe the rate of change of this expectation value consequent upon the collision. To include this case in the theorem, $A_1(\alpha)$ is replaced everywhere by

$$\sum_b P_{b,1} A_1(\alpha) P_{b,1}. \tag{17}$$

Although the resulting analytical expressions are even more difficult to evaluate than those obtained previously, they do confirm that the most general physical measurement conceptually possible can be accomodated into the theorem.

To include the Pauli principle, we use the same state vectors used thus far—in which the particles are distinguishable—but the wave packet in (3) is replaced by $s\Psi_{a,1}^{(+)}$, where s is the appropriate symmetrization or antisymmetrization operator.

The closed expressions that must be evaluated in connection with the generalized Ehrenfest theorem appear too complicated for practical application. Instead, it appears that the real usefulness of the theorem is to enable the physical properties of the scattering process to be simply and directly defined in terms of the mathematical formalism, as was done here, for example, in calculating $w_{b,c;a,1}$. A development of collision theory from this point of view will be published elsewhere.

*This work was supported by the Advanced Research Projects Agency.

[1]B. A. Lippmann, in Abstracts of Papers of the Fourth International Conference on the Physics of Electronic and Atomic Collisions (Science Bookcrafters, Inc., Hastings-on-Hudson, New York, 1965), p. 210 (time-dependent theory); B. A. Lippmann, Phys. Rev. Letters 15, 11 (1965) (time-independent theory).

[2]See B. A. Lippmann, Phys. Rev. 102, 264 (1956), Eq. (3.12).

[3]See, for example, the discussion in L. D. Landau and E. M. Lifshitz, Quantum Mechanics (Pergamon Press, New York, 1958), p. 60.

ELECTRONS IN THE PLASMA SHEET OF THE EARTH'S MAGNETIC TAIL*

S. J. Bame, J. R. Asbridge, H. E. Felthauser, R. A. Olson, and I. B. Strong

Los Alamos Scientific Laboratory, Los Alamos, New Mexico

(Received 19 November 1965)

Magnetic field measurements made from satellites in recent years[1-3] have demonstrated that beyond the Van Allen trapping region on the dark side of the earth, the geomagnetic field is stretched radially outward in the antisolar direction, and forms a magnetic tail extending beyond 31 earth radii. The measurements of Ness[3] on IMP-1 showed that a region of field reversal existed between regions of oppositely directed field lines stretched from the magnetic polar regions into the tail. On some of the IMP-1 passes, the magnitude of the field decreased to values near zero and the direction reversed over a narrow spatial range, showing the existence of a "field-free surface" in the tail. On other passes the field reversal occurred over a more extended range; examples of multiple reversals were also observed. Explorer 14 and EGO-1 measurements also showed dramatic examples of abrupt field reversal over a narrow spatial range. However, reversal over a more extended range was more commonly observed, often with the field magnitude remaining at appreciable values throughout the reversal.[4]

The magnetospheric-tail model of Axford, Petschek, and Siscoe[5] has a relatively thick "neutral sheet" region of field reversal at the radial distances of the measurements reported here. In their model an enhanced plasma containing low-energy electrons is expected in the region of field reversal to supply particle pressure which prevents the collapse of the field configuration. Thus, it is to be expected

that a "plasma sheet" associated with the "neutral sheet" should exist in the tail.

Early measurements of low-energy electrons made in the tail[6,7] have been summarized by Van Allen.[8] Flux values of 10^8-10^9 cm^{-2} sec^{-1} were found for electrons with $E > 200$ eV. Higher energy electrons also have been found in the tail[9-12] and shown to be located about an extension of the plane of the geomagnetic equator.[9,11,13] Electrons with energies above 45 keV appear and disappear in an impulsive manner, often with fast-rising intensities, and slower decays.[10] It seems clear that these individual electron "islands" are not permanent features in a spatial sense, but the sources and nature of the energetic electron events have not been completely deduced.

Simultaneous measurements of low-energy electrons ($0.35 \leq E \leq 20$ keV) and energetic electrons ($E > 45$ keV) have been made on the Launch-2 Vela satellites[14] in the tail of the magnetosphere between 16 and 18 R_E. Some of the major results to be reported here follow: The electron component of a plasma sheet has been observed. The plasma sheet is located in the expected region of field reversal, or "neutral sheet," and often has a thickness of $6R_E$ or more at $17R_E$. The electrons have quasithermal energy distributions and energy densities comparable to the expected magnetic field energy densities. The observed energetic electrons are ordinarily contained in the high-energy tails of the energy distributions. Impulsive energization of the electron population is a common feature of the plasma sheet, resulting in rapid increases in the energetic electron flux.

Low-energy electron fluxes are measured with an electrostatic analyzer at 14 energy levels; energetic electron fluxes are measured with a thin-window Geiger counter (EON 6213). Measurements are made simultaneously with both detectors, once per second, covering 5 equally spaced angles within ±12° of the vehicle-sun line, and one each in the general direction of the dusk meridian, the antisolar direction, and the dawn meridian. Omnidirectional fluxes are obtained by integrating over the energy and angular distributions of the analyzer and over the angular distributions of the Geiger counter.

In September-October 1964 the satellites passed through the magnetospheric tail near the antisolar point 22 times. Data from part of the pass of 4-5 October 1964, during a period of moderately high geomagnetic activity, have been selected to illustrate some of the important features which have become apparent, and are shown in Fig. 1. Throughout the time history, the angular distributions of the electrons were generally close to isotropic, except for a significant streaming of energetic electrons[13] near 0200 UT. As the spacecraft descended from high latitudes toward the cen-

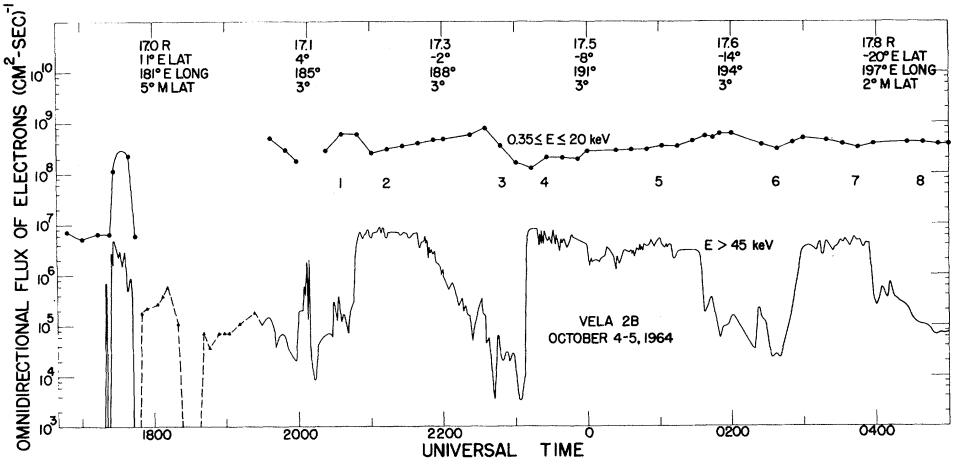

FIG. 1. Time history of omnidirectional fluxes of electrons for a portion of a pass through the tail of the magnetosphere. Electron flux with $0.35 \leq E \leq 20$ keV is measured with an electrostatic analyzer; flux with $E > 45$ keV is measured with a thin-window Geiger counter. Radial distance, ecliptic latitude and longitude, and geomagnetic latitude of the spacecraft are given at the top of the graph. Analyzer data are not available for those times without points. Integral energy spectra for the numbered times are given in Fig. 2.

ter of the magnetospheric tail, the first fluxes above the background levels of both high- and low-energy electrons were observed in the short event at 1730 UT. Both high- and low-energy fluxes rose and fell together. On the other hand, at 2050 UT the energetic flux rose sharply by two decades in 4 minutes to flux values near the highest which have been observed on the Vela-2 satellites, while the flux of low-energy electrons did not change in a corresponding way. Indeed, throughout the time history shown, the low-energy flux values seem to bear little relationship to the high-energy flux, except for the event at 1730 UT. After 2100 UT the low-energy flux remained within the range of 10^8 to 8×10^8 cm^{-2} sec^{-1}, while the energetic flux varied by three decades or more. The energetic events appear to have the characteristics of the island fluxes observed by Anderson.[10,11]

Integral energy distributions of the electrons are shown in Fig. 2 for the numbered times in Fig. 1. The 45-keV points fit power-law extrapolations of the analyzer spectra. The power-law exponents lie between −2.7 and −3.5, in general agreement with the range of exponents given by Montgomery et al.[9] for electrons above 50 keV. The counting statistics are not an important source of error. However, the absolute flux values of the analyzer are thought to have an accuracy no better than ±50%; the 45-keV threshold value of the Geiger counter is nominal and not considered highly accurate. Nevertheless, it seems apparent that the energetic electrons are a part of a high-energy tail of electrons with an energy distribution which has a single functional form. The large fluctuations in energetic flux are caused by changes in the energy spectrum of the total electron population.

The energy spectra have a broad quasithermal character which is flatter than a pure thermal distribution. Some of the parameters derived from the spectra are presented in Table I. Fluctuations in the average energy correlate with fluctuations in the energetic electron flux values. The average energy would correspond to twice the temperature if the distributions were Maxwellian.

The electron densities shown in the table are lower for the higher average energies. This may be explainable in part because of the greater pressure exerted by higher energy electrons on the magnetic field, causing the volume containing the particles to expand with a resulting drop in particle density.

If it is assumed that the positive ions in the plasma have the same energy density as the electrons, equating magnetic field energy density with kinetic-energy density of the particles yields the magnetic field intensity values shown in Table I. These values lie within the measured field values which range from very weak or zero to more than 30×10^{-5} G in the region of field reversal.[3,4] Thus, it seems that the electrons are the electron component of the enhanced plasma which provides the required particle pressure in the region of field rever-

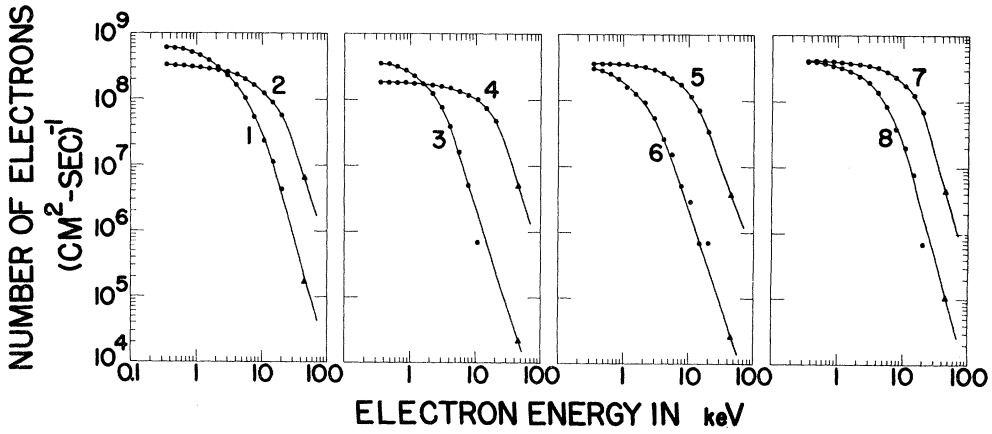

FIG. 2. Integral energy spectra of electrons determined at the numbered times of Fig. 1. Points below 20 keV are determined with an electrostatic analyzer, the points at 45 keV with a Geiger counter. Large increases in electron flux for $E > 45$ keV seem to be caused by an impulsive change in the energy distribution of the total electron population.

Table I. Average energy, electron density, electron energy density, and magnetic field intensity required to yield magnetic field energy density of twice the electron energy density, for the spectra in Fig. 2.

Spectrum	Average energy (keV)	Electron density (cm^{-3})	Energy density (10^{-9} erg cm^{-3})	B (10^{-5} G)
1	3.0	0.23	0.66	18
2	8.2	0.08	0.61	18
3	1.7	0.18	0.34	13
4	12.0	0.04	0.49	16
5	8.3	0.08	0.75	14
6	1.4	0.19	0.26	11
7	10.3	0.09	1.0	22
8	3.1	0.17	0.51	16

sal. The omnidirectional fluxes generally range between 10^8-10^9 electrons cm^{-2} sec^{-1}.

The enhanced plasma forms a sheet extending across the magnetospheric tail. The measurements show that ordinarily the low-energy electrons are found in the same regions occupied by the energetic electrons. Thus, other measurements of the spatial distribution of the band of energetic electrons[9,11-13] lying across the magnetospheric tail can be used as a general indication of the location and thickness of the plasma sheet. The Vela-1 measurements[9] show the sheet often to be at least $6R_E$ thick near the antisolar point at $\sim 17R_E$. Further analysis of the spatial distribution of the low-energy electrons is continuing.

Within the plasma a fast rise in energetic electron flux can often be interpreted as an impulsive energization or heating of the entire electron population. The slower decrease in energetic flux reflects a decrease in the average energy of the electrons, which may be caused by one or more of the following: a more rapid diffusion of energetic electrons away from the region, a streaming of energetic electrons away from the region,[13] a cooling of the electrons, a drift of the region with a given average energy away from the spacecraft, or the movement of the spacecraft out of the region.

In regions near the plasma-sheet boundaries, movements of the boundaries could produce sudden changes in the total electron population. The event at 1730 UT could have been caused in this manner. Inside the plasma sheet, energetic flux events with slow rise times are also observed, and may be caused by diffusion and drifting of regions in which the electrons have different average energies. Spacecraft motion through different regions can also be a factor for slowly varying flux histories.

The Vela results, as well as those of Anderson,[10,11] show that energetic fluxes often decay rapidly after a period of slow decay as seen at 0135 UT. The integral energy spectra, Nos. 5 and 6, demonstrate that the spectrum has softened during this time. This feature suggests that impulsive de-energization or cooling of the electron population can also occur.

---

*Payload and data analysis responsibilities were carried out at the Los Alamos Scientific Laboratory under auspices of the U. S. Atomic Energy Commission, and the program was otherwise supported by the Advanced Research Projects Agency, the U. S. Air Force Space Systems Division, and the U. S. Atomic Energy Commission.

[1]J. P. Heppner, N. F. Ness, C. S. Scearce, and T. L. Skillman, J. Geophys. Res. 68, 1 (1963).

[2]L. J. Cahill, Jr., Trans. Am. Geophys. Union 45, 231 (1964).

[3]N. F. Ness, J. Geophys. Res. 70, 2989 (1965).

[4]L. J. Cahill, Jr., in Proceedings of the International Space Science Symposium (COSPAR), 1965 (to be published), and J. P. Heppner, Goddard Space Flight Center Report No. X-612-65-490, presentation at the ESRO Colloquium, Stockholm, Sweden, 1965 (to be published).

[5]W. I. Axford, H. E. Petschek, and G. L. Siscoe, J. Geophys. Res. 70, 1231 (1965).

[6]K. I. Gringauz, V. V. Bezrukikh, V. D. Ozerov, and R. E. Rybchinskii, Dokl. Akad. Nauk SSSR 131, 1301 (1960) [translation: Soviet Phys.—Doklady 5, 361 (1960)].

[7]J. W. Freeman, J. Geophys. Res. 69, 1691 (1964).

[8]J. A. Van Allen, J. Geophys. Res. 69, 1011 (1964).

[9]M. D. Montgomery, S. Singer, J. P. Conner, and E. E. Stogsdill, Phys. Rev. Letters 14, 209 (1965).

[10]K. A. Anderson, Phys. Rev. Letters 14, 888 (1965).

[11]K. A. Anderson, J. Geophys. Res. 70, 4741 (1965).
[12]L. A. Frank, J. Geophys. Res. 70, 1593 (1965).
[13]Evidence for streaming of energetic electrons outward from the earthward direction and their spatial distribution is presented in J. R. Asbridge, S. J. Bame, H. E. Felthauser, R. A. Olson, and I. B. Strong, Trans. Am. Geophys. Union 46, 142 (1965).
[14]The second launch of twin Vela nuclear test detection satellites occurred on 17 July 1964. Details of the orbits and instrumental characteristics can be found in a series of abstracts in Trans. Am. Geophys. Union 45, 623 (1964).

SPECTRUM OF CRAB NEBULA X RAYS TO 120 keV

Laurence E. Peterson, Allan S. Jacobson, and R. M. Pelling
Physics Department, University of California, San Diego, La Jolla, California
(Received 27 December 1965)

In this Letter, we wish to report a balloon determination of the Crab nebula x-ray spectrum over the range 16 to 120 keV. X rays from the Crab were first discovered from a rocket,[1] and were observed from a balloon to 60 keV by Clark.[2] In this work the spectrum has been extended and determined to a much higher precision.

The detector[3] consists of a NaI crystal 5 mm thick by 24-mm diameter. Collimation is provided by a cylindrical CsI scintillation cup 9.3 cm o.d. by 22.9 cm long with a 2-cm wall which surrounds the central detector and its phototube. This collimator, which is in anticoincidence with the central detector, also rejects background events produced by cosmic rays. The detector area is 9.4 cm^2, its geometry factor is 1.5 cm^2 sr, and its resolution, full width at half-maximum, 54%, at 30 keV. Postflight and preflight energy calibrations were identical. In-flight calibrations during a previous flight with the same apparatus showed no tendency for gain changes. Data were telemetered event by event in a digital format from a 128-channel pulse-height analyzer. The detector was mounted at a fixed elevation of 80°, and servo-controlled in azimuth to point true south. The reference was obtained from a magnetometer set to compensate for the average magnetic declination over Texas. The azimuth was independently verified to within about a degree by two additional crossed magnetometers.

The balloon was launched from Palestine, Texas, at 2234 CST, 23 September 1965, reached ceiling at 0050 CST, and floated level at 3.3 g/cm^2 until 0610 CST, when the instrument was inadvertently released by radio command. The Crab transit on this date, corrected for the drift in longitudes of the balloon, was 0545 CST.

Figure 1 shows the counting rates as a function of time for various energy ranges, averaged over 12-minute intervals. The peak on ascent is due to the cosmic-ray maximum. The rate increase at lower energies as the balloon approaches ceiling is apparently due to a diffuse component of cosmic photons. This flux, when corrected to zero depth, seems

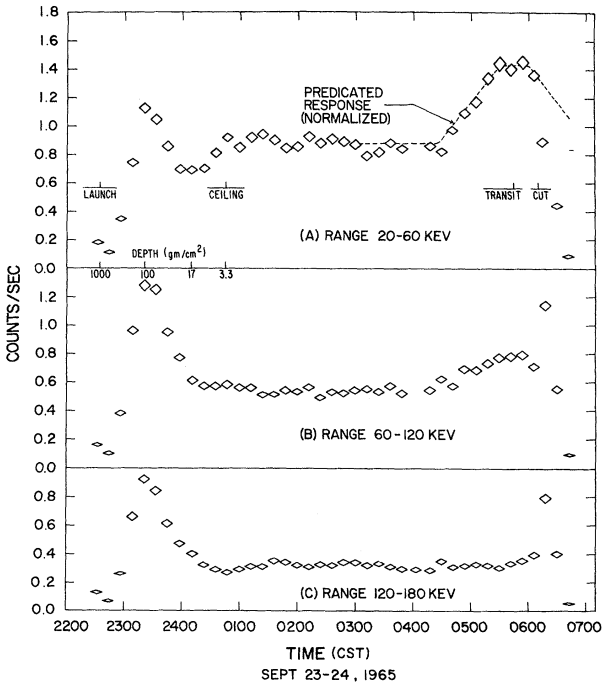

FIG. 1. The counting rates at various energy ranges as a function of time. Background data were obtained at ceiling before the meridian transit of the x-ray source. The dashed line shows the expected transit profile for a point source at the position of the Crab nebula.